Membrane and Water Treatment, *Vol. 13, No. 4 (2022) 173-181*
https://doi.org/10.12989/mwt.2022.13.4.173

Morphological study of synthesized PVDF membrane using different non-solvents for coagulation

Meenakshi Yadav, Sushant Upadhyay*, Kailash Singh,
Tarun Kumar Chaturvedi and Manish Vashishtha

Department of Chemical Engineering, Malaviya National Institute of Technology Jaipur-302017, India

(Received February 4, 2022, Revised May 27, 2022, Accepted May 31, 2022)

Abstract. Polyvinylidene fluoride (PVDF) flat sheet hydrophobic membranes were prepared using 16 wt% PVDF in Dimethyl acetamide (DMAc) by phase inversion technique for desalination application using Membrane Distillation (MD). In this work, the effect of coagulation mediums such as ethanol and water as well their synergistic behavior on the fabricated PVDF membrane morphology was studied using SEM. Moreover, other characteristics required for the membrane distillation applications namely porosity, hydrophobicity and tensile strength were measured using the gravimetric method, sessile drop method and universal testing machine respectively. It was observed that the membrane morphology paradigm shifted from the finger-like structure to the sponge-like structure on increasing the ethanol concentration in coagulant. The porosity of the fabricated membrane was under the required MD range and found to be 57.3% at 16 weight % of PVDF in DMAc solvent under a pure ethanol coagulant bath. Moreover, the top surface contact angle ranges from 85° to 115° on increasing the bath concentration from CBC 0 to CBC 100 at 16 weight % of PVDF in DMAc solvent.
Keywords: polymers; membrane distillation; membrane property; membrane fabrication

1. Introduction

Membrane technology has gained an important role in the separation process because of its wide range of applications using various membrane processes such as microfiltration (MF), ultrafiltration (UF), nanofiltration (NF), reverse osmosis (RO) and membrane distillation (MD). The latter is a frontier membrane technology and gained interest as it has the potential for desalinating highly saline water with rejections of ions and other non-volatiles with less energy consumption and a higher value of selectivity (Macedonio *et al*. 2010, Baghel *et al*. 2017, Singh *et al*. 2017). The choice of the membrane is the key factor that determines the performance of the membrane process, for MD application. The prime feature of the membrane for MD application is hydrophobicity. The hydrophobic membrane used in MD processes acts as a physical barrier to prevent the liquid feed entering into membrane pores and allowing only vapors to pass through the membrane. (Baghel *et al*. 2020, Gryta 2010). A liquid-gas interface was developed by the membrane in MD which plays a vital role in understating the heat and mass transfer phenomena across the membrane (Upadhyaya *et al*. 2016b).

The membrane properties play a key role in membrane-based water treatment processes and determine the technological as well as economic efficiency of the aforementioned technologies, therefore, it is obvious membrane improvement can greatly affect the performance of current technology. Porosity, hydrophobicity and morphology are the major characteristics of the membrane that define its performance in membrane processes. The material selection and pore size of the membranes depend on the application for which they would be used in the MD. Polyvinylidene fluoride (PVDF), polypropylene (PP) and polytetrafluoroethylene (PTFE) are the major polymers that are generally used by researchers to prepare hydrophobic MD membranes, among them PVDF has gained the great interest because of its greater thermal stability and chemical resistance to reagents like acids, bases and organic solvents (Garcia-Payo *et al*. 2010, Sui *et al*. 2012, Zhang *et al*. 2011, Zhu *et al*. 2013, Tibi *et al*. 2020). Numerous authors (Peydayesh *et al*. 2020, Gholami *et al*. 2013, Haan *et al*. 2018) have used different methods and polymers to prepare the various types of the membranes. In the literature, hydrophobic membranes such as poly tetra fluoro ethylene (PTFE) and poly-sulphone (PSF) were rapidly used for the Membrane Distillation process due to their excellent chemical and mechanical resistivity (Eykens *et al*. 2017, Upadhyaya *et al*. 2016a, Marino *et al*. 2018). However, these membranes are not effective to produce high permeate flux. Therefore, some other alternatives yet need to be explored in terms of another suitable polymer that not only provides adequate hydrophobicity but also high flux for MD applications. The inherent hydrophobicity of PVDF polymer is not as higher as PTFE however its hydrophobicity can be increased by slowing the rate of liquid-liquid demixing without compromising its porosity (Chang *et al*. 2014). Therefore, it can be attributed that polymer selection is not only the choice for deciding factor of membrane properties but its casting process also affects its characteristics. Researchers have investigated that there is a wide gap between the crystallization line and binodal curve

*Corresponding author, Ph.D.,
E-mail: supadhyay.chem@mnit.ac.in

ISSN: 2005-8624 (Print), 2092-7037 (Online)

for the phase diagram drawn for PVDF- DMF- alcohol than that for the phase diagram of PVDF- DMF- water, this shows the possibility of crystallization/ gelation of PVDF dominates the membrane structure (Pagliero *et al*. 2020). However, the bath composition effect on membrane characteristics is overlooked in the literature. But in the opinion, during the non-solvent induced phase separation process (NIPS), the interaction rate between coagulation bath and solvent may get different if the coagulation medium composition is varied. In order to obtain an appropriate membrane with desired properties, the bath composition effect may also be taken into account otherwise, few of the characteristics of the membrane are not in a desired range suitable for MD applications. Yadav *et al*. (2021) have discussed the effect of coagulation medium temperature on PVDF membrane characteristics such as membrane morphology, porosity and contact angle however, the simultaneous effect of coagulation medium composition is overlooked. Certainly, extensive study to understand the effect of coagulation medium composition on membrane morphology and other desired properties is yet to be deeply explored. Therefore, in this work, the effect of different non-solvent such as water and ethanol with their varied composition was extensively investigated to understand its effects on synthesized PVDF membrane characteristics using NIPS. The level of hydrophobicity is generally understood by the authors (Li *et al*. 2011, Hou *et al*. 2009) by estimating the contact angle however, to deepen the knowledge surface roughness of the synthesized PVDF membrane was also corroborated in this work by capturing the image using Atomic Force Microscope beside contact angle.

2. Materials and experimental methods

In this section, chemicals procured and the experimental procedures for membrane casting are described.

2.1 Materials

Commercially available polyvinylidene fluoride PVDF, FR-904 (MW= 444000, Sita chemicals Pvt., Ltd. India) was used as membrane material and Dimethyl acetamide (DMAc) (99.5% AR grade, density = 0.940 g/ml, TECH INC India Pvt) was used to prepare the polymeric solution. Ethanol (AR grade, Merck, Savita Chemical Co., Ltd. (India)) was used as an external coagulation bath along with the double distilled water which was prepared by a double distillation unit in the advanced polymer processing lab. A non-woven fabric (0.1 mm thick) was purchased from the Permionics Membranes Pvt. Ltd, Vadodara, Gujarat and used as membrane support at the time of film casting to avoid shrinkage during the drying operation.

2.2 Membrane preparation

Firstly a homogeneous dope solution was prepared by mixing PVDF powder (16 wt % of the total solution) with the DMAc solvent. The mixture was then kept on a temperature control magnetic stirrer that was maintained at 700°C for 24 hours to obtain a homogeneous solution. The polymeric dope solution was kept in a glass bottle and degassed for 24 hours. Afterward, this dope solution was used to prepare polymeric membranes by the non-solvent induced phase separation (NIPS) a well-known process to prepare asymmetrical membranes. In brief, a sheet of non-woven fabric was cut in a particular dimension to get fixed over a glass plate to provide a smooth surface for membrane casting. After that glass plate was fixed on the membrane casting machine and the gap between the sheet and blade was maintained to be 250-µm, so that membrane with a uniform thickness could be cast. Thereafter, about 10 ml of dope solution was uniformly poured into the channel provided near the blade in the casting machine, the blade was pulled out with a uniform speed throughout the glass plate, casting the membrane on non-woven fabric. This thin polymeric film on the non-woven fabric along with the glass plate was poured into a coagulation bath. The configuration of the non-solvent bath was varied from 0 wt % ethanol to the 100 wt % ethanol in the ethanol-water mixture as given in Table 1. The immersion process was carried out at room temperature for 24 hours. Any remaining solvent was completely removed by soaking in double distilled water for 24 hours. After removal of solvent from membrane matrix, the membrane was dried at room temperature for 2 days and stored for further characterization. The process of dope solution preparation and casting of the membrane was shown in Fig. 1.

2.3 Membrane characterization

Different characterization techniques were used to characterize the hydrophobic membrane, like the Gravimetric method, sessile drop method, atomic force microscopy (AFM) and universal testing machine (UTM) were used to determine the porosity, contact angle, surface roughness and tensile strength of the casted membranes. Morphology of the membrane was observed by Scanning electron microscope (SEM).

2.3.1 Porosity

Membrane porosity (ε) is defined as the volume of the pores divided by the total volume of the microporous membrane. It can be determined by, the gravimetric method (Abdel-karim *et al*. 2018, Munirasu *et al*. 2017), which determines the weight of liquid contained in the membrane pores. We used isopropyl alcohol whose surface tension was 23.00 mN/m @ 25°C for its low surface energy. Membrane coupons were cut and dipped in isopropyl alcohol overnight so that it can penetrate completely inside the pores of the membrane. Thereafter, the weight of each sample of membranes was measured on the analytical balance up to 3-digit precision after the decimal. Each sample of the membrane was measured four times to avoid error and then an average of them was used to estimate the porosity, by using Eq. (1) (Xu *et al*. 2019).

$$\varepsilon = \frac{\frac{(w_w - w_d)}{D_i}}{\frac{(w_w - w_d)}{D_i} + \frac{w_d}{D_p}} \quad (1)$$

where w_w -weight of wet membrane(g), w_d - weight of

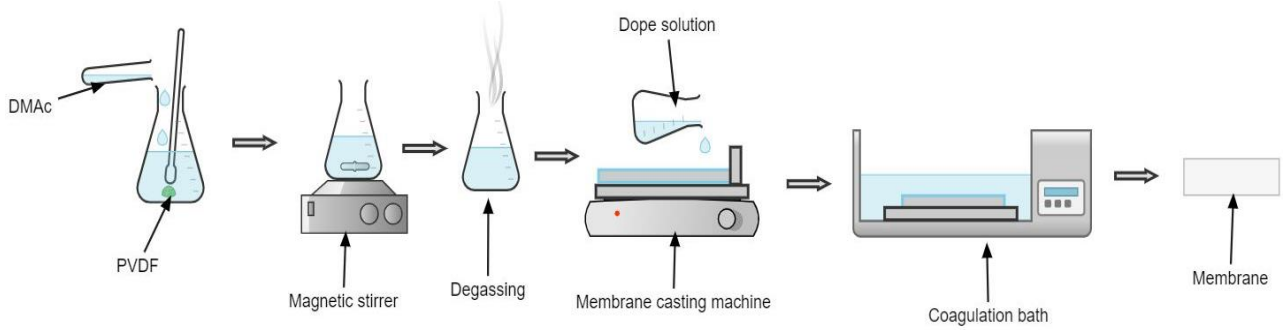

Fig. 1 Pictorial presentation of membrane preparation technique

Table 1 Membrane code and composition of its non-solvent coagulation bath [PVDF = 16 wt%, DMAc = 84 wt% of total casting solution]

Membrane code	Ethanol % in coagulation medium	Water% in coagulation medium
CBC-0	0	100
CBC-15	15	85
CBC- 30	30	70
CBC- 45	45	55
CBC- 60	60	40
CBC-75	75	25
CBC-100	100	0

dry membrane(g), D_i - isopropanol density in g/m^3 and D_p - polymeric membrane density in g/m^3, respectively.

2.3.2 Static contact angle

The static Contact angle (θ) between water and PVDF microporous membrane was measured to evaluate the membrane hydrophobicity by the sessile drop method with a Drop Shape Analyzer (DSA25) Mk2 of firm Kruss, Germany. A water droplet of 10 µl was carefully dropped on the surface of membrane square coupons and contact angles were determined in 10 sec after the water was dropped and without apparent change in CA. A lens and a source light were used to create the drop image on a screen. The contact angle was determined with the projected drop image. Five different spots for each sample were measured. The average value of the five spots as the contact angle of the membrane sample was used as an output to minimize the error.

2.3.3 Atomic force microscopy (AFM)

Membrane surface roughness was measured by atomic force microscopy (AFM, Veeco Dimension Icon) in the tapping mode under ambient conditions using commercially available Si cantilevers (300 kHz frequency). The force constant of the cantilevers was 40 N/m. The oscillation frequency used for tapping mode was 310±5 kHz. The scan rate of 1.0 Hz was used with a scan size of 5×5 mm.

2.3.4 Liquid entering pressure (LEP)

The LEP value of the synthesized membrane was measured using dead-end filtration setup. At the feed side, NaCl solution was filled and pressure was increased stepwise using compressed nitrogen gas until NaCl solution penetrates through the membrane. Penetration of NaCl was detected by a conductivity meter. The pressure at which the first drop of NaCl pass through the membrane was considered as LEP of that particular membrane.

2.3.5 Mechanical properties

Mechanical properties like Tensile strengths and elongations at the breaks of the membranes were measured using Universal Testing Machine (UTM) at room temperature. The membrane was cut in rectangular strips of dimension 10 cm × 2 cm, with a margin of 1.5 cm on both sides to clamp the sample in the machine. These samples were clamped at both ends and pulled in tension at a constant elongation rate of 10 mm/min, gauge length 50 mm and maximum force 250 N. For each condition used, we report the average value of at least three tests.

2.3.6 Morphology study

The morphologies of the surface and the cross-section of the membranes were examined using scanning electron microscopy (SEM, FEI, Quanta200) to understand the overall microstructure of the membrane for better flux in MD configurations. The dry membrane samples were frozen in liquid nitrogen and then fractured to expose the cross-sectional areas. These fractured membranes were deposited on the copper holder and their cross-sectional surface was gold-sputtered to make them conductive. Then they were transferred to the SEM where their images at different magnifications were captured to study the change in morphology of the membrane by varying the coagulation bath configuration.

3. Result and discussion

In this section, the effect of non-solvent coagulation baths such as water, ethanol and the mixture of both on casted PVDF membrane morphology was investigated for better understanding. Moreover, the effect of non-solvent concentration on membrane porosity, contact angle and tensile strength was also studied for PVDF membrane.

3.1 Effect of coagulation bath on membrane morphology

SEM micrographs of the PVDF flat sheet membrane under various coagulant bath concentrations ranging from

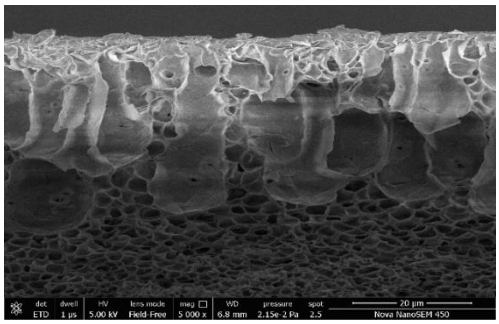

(a) CBC-0

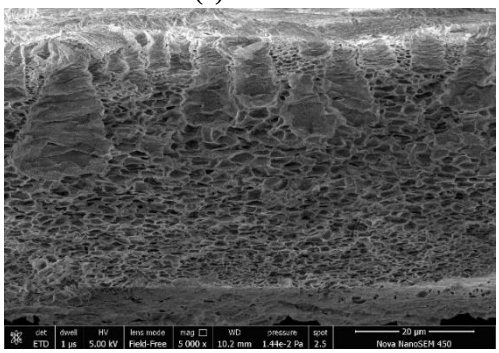

(b) CBC-15

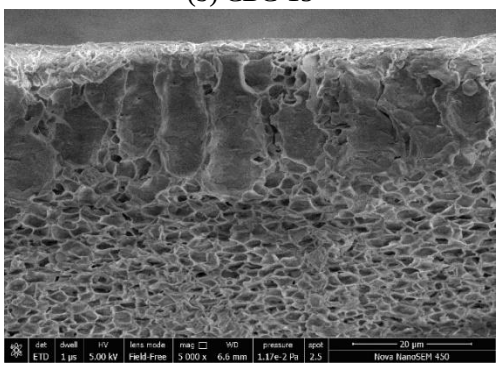

(c) CBC-30

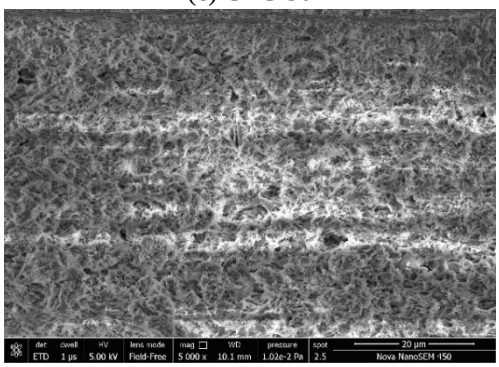

(d) CBC-100

Fig. 2 Cross-sectional micrograph of casted PVDF membrane with different coagulation bath concentration (at magnification 5000)

CBC-0 to CBC-100 as per the composition mentioned in Table 1, are shown in Figs. 2(a)-2(d). It is clearly seen from the micrographs of Fig. 2(a) that near the top surface of the membrane long finger-like structures are found present and at the bottom sponge-like structures are depicted. This structure of the polymeric membrane can be attributed to the fact that rapid demixing may have occurred at the top surface of the polymeric film in the coagulation medium, as a result, interdiffusion between solvent/non-solvent will get faster which in turn binodal gap may be reached quickly. Therefore, it can be corroborated, when the water percentage in coagulant is 100% (CBC-0), the liquid-liquid demixing dominates, leading to a cellular morphology due to which the pores grow in the polymer lean phase and are embedded in the solid polymeric matrix. From Fig. 2(a), it can be visualized that three sequential regions of different morphology reflect a thin polymeric layer at the top surface, underneath a finger-shaped macro void layer and at the last bottom lose-packed globules (sponge-like morphology). The reason for sponge globules in the extreme last layer is due to the fact that the thin top layer, as well as the thickness of the middle layer, restricts the inter diffusive transport of solvent to get a transfer from the membrane matrix to the coagulant bath. This results in crystallization before liquid-liquid demixing.

However, in the SEM micrograph of CBC- 15 (15 wt% ethanol in an ethanol-water mixture) represented in Fig. 2(b), it is seen that the length of finger-like microvoids at top of the membrane matrix gets reduced as compared to Fig. 2(a). This is because, the solvent – nonsolvent diffusion rate may not be as fast as compared in the previous case due to the addition of ethanol in the bath. Furthermore, a decrement in the length of finger-like pores can be observed in Fig. 2(c) on increasing the ethanol concentration from CBC 15 to CBC 30. This clearly proclaims that the addition of ethanol in the coagulation bath lowers the strength of non-solvent, due to which driving force to mass transfer decreases which in turn depressed the liquid-liquid demixing rate.

On further increasing the ethanol concentration to 100 wt % (CBC-100), it is observed from Fig. 2(d) that the morphology of the membrane shifted towards interconnected spherulites of small dimensions with no macro voids present in the membrane matrix. This is because the solvent-non-solvent exchange rate dropped at a higher concentration of ethanol in the bath medium due to which membrane formation took a long time and hence creating a more symmetric structure where macro voids gradually disappeared. Moreover, a bicontinuous structure can be visualized easily in Fig. 2(d). This happens due to the crystallization-dominated process prior to liquid-liquid demixing. In this situation, the distance between the crystallization and the binodal lines increased further so that all crystalline particles were allowed to grow and coalesce to form a bicontinuous structure.

Finally, it is corroborated that when the concentration of ethanol varies from CBC-0 to CBC-100 in a coagulation bath then membrane morphological structure shifts from finger to the sponge-like structure. This is mainly mainly due to the fact of thermodynamic and kinetic factors during NIPS. The solubility of water (strong non-solvent) in solvent (DMAc) is more as compared to the solubility of ethanol (week non-solvent) in solvent (DMAc) therefore, the exchange rate for CBC-0 is higher as compared to CBC-100 during the phase inversion process. This kinetic mechanism of mutual transfer of solvent and non-solvent (either ethanol or water) affects the mass transfer rate as a

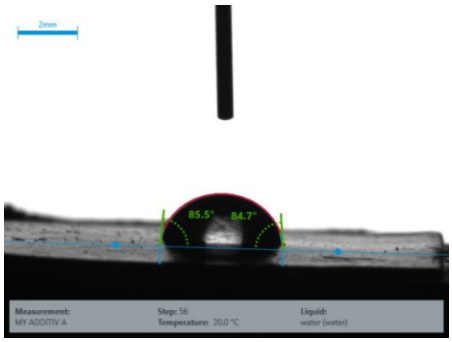

(a) CBC-0

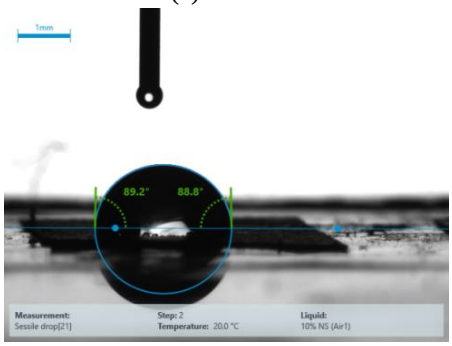

(b) CBC-15

(c) CBC-30

(d) CBC-100

Fig. 3 Contact angle of casted PVDF membrane with different coagulation bath concentrations

result of changes in morphological structure. Fundamentally, the mass transfer is proportional to the concentration difference of the components in both phases wherein, this difference is more between water and DMAc as compared to ethanol and DMAc due to the solubility difference factor. Therefore, when a strong non-solvent as the water was used (CBC-0) as a coagulation medium, the mass transfer difference will be greater which promotes instantaneous demixing of solvent and non-solvent (water), resulting in a deeper figure like pores in the membrane. For achieving high flux, a deepen finger-like structure is required in the top layer followed by a sponge-like structure at the bottom layer of the membrane for good support and strength. Therefore, a trade-off between coagulant bath concentration is to explore thoroughly by varying its concentration. Moreover, this trade can also be improved by varying the additive and solvent concentration during dope solution preparation. It is noteworthy that on varying the dope solution concentration the degree of shift of the binodal line in the phase diagram may shift either polymer-solvent or polymer-non-solvent phase line which ultimately alters the thermodynamic instability of the casting solution which in turn may affect the membrane morphology.

Table 2 Water contact angle measured on the top surface of 16 wt% PVDF membrane at different coagulation bath compositions

Membrane code	Water Contact Angle (º)
CBC-0	85º ± 5°
CBC-15	89º± 5°
CBC- 30	92º± 5°
CBC- 45	97º± 5°
CBC- 60	103º± 5°
CBC-75	109º± 5°
CBC-100	115º± 5°

From the SEM morphology represented in Fig. 2, it can be corroborated that during phase inversion, the coagulation medium plays a very specific role in the formation of the membrane. Generally, the solubility parameter is the deciding factor for the rate of demixing of solvent and non-solvent. Water presents better coagulation ability which increases the precipitation rate during the phase inversion process and thereby instantaneous demixing occurs. Moreover, the fast coagulation rate results in the formation of large finger-like macro voids and cavities like structure, that is, after immersion of polymeric film, a dense skin layer is formed, which acts as a barrier for diffusion of the coagulation medium, inwards and the solvent out from the casting solution.

3.2 Effect of coagulation bath on membrane hydrophobicity and LEP

The top surface contact angles images of PVDF membranes which were prepared using different coagulant bath compositions are captured and represented in Fig. 3. The values of contact angles along with their standard deviation are shown in Table 2. It is observed from Table 2 that on increasing the percentage of ethanol in the coagulation bath, the surface contact angle of the membrane increases from 85˚ to 115˚. This may be explained by the fact that water acts as a strong non-solvent and result in the formation of a smooth thin layer of polymer on the top of the membrane as shown in Fig. 4(a), but with the addition of ethanol, liquid-liquid demixing get delayed and poly-

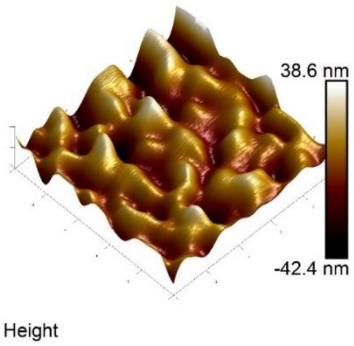

(a)

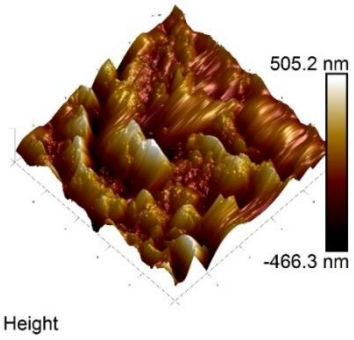

(b)

Fig. 4 Three-dimensional AFM topographical surface images of the membranes: (a) CBC-0 and (b) CBC-100

Table 3 LEP measured of 16 wt % PVDF membrane at different coagulation bath compositions

Membrane code	Experimental LEP (kPa)	Theoritical LEP (kPa)
CBC-0	92.10	-
CBC-15	112.72	-
CBC- 30	123.45	109.67
CBC- 45	144.11	123.42
CBC- 60	156.34	145.75
CBC-75	165.87	158.65
CBC-100	189.92	172.43

merization of membrane starts prior to precipitation. Some researchers (Li *et al*. 2011, Deshmukh and Li 1998) claimed, that when ethanol in coagulant became dominating, the top layer of the membrane polymerized to form a hydrophobic surface.

Wenzel and Cassie-Baxter, are two wetting theories states generally based on the way the water droplet rests on a rough surface. The assumption of the Wenzel model was that the liquid wets the whole rough substrate, while in the case of the Cassie-Baxter model assumption, the droplet partially wets the rough substrate due to the trapped air in the micro-structured surfaces. The Cassie Baxter equation was more generally used to evaluate the contact angle of drop placed on a flat composite micro heterogeneous surface:

$$Cos\ \Theta_{CB} = -1 + (1 + r_f\ Cos\ \Theta) \times f \qquad (2)$$

where, Θ_{CB} is contact angle and f is the surface fraction occupied by solid in a composite flat surface made of solid with trapped air pockets. For the membrane under investigation, it is found that on increasing the ethanol concentration in the coagulation bath, f decreases, that is the number of solid fraction decreases and more surface was occupied by the air pocket, resulting in an increase in contact angle. This can also be defined as surface roughness and with an increase in surface roughness, surface hydrophobicity increases (Essalhi and Khayet 2012, Kotsilkova *et al*. 2018).

The membrane wetting phenomena play a crucial role in MD membrane characteristics. Besides contact angle, in order to understand the wetting phenomena, another hydrodynamic characteristic is known as Liquid Entry Pressure (LEP) also plays a significant role to understand the pore wetting phenomena. LEP is defined as the maximum trans membrane pressure applied to the membrane above which, a liquid droplet of feed pass through the pores of the membrane. When the trans membrane flux exceeds the LEP, the feed solution will flood the membrane pore(s) and the selectivity of flux through membrane distillation decreases. The young-Laplace equation as represented in Eq. (3), is the most frequently used model equation found in the MD literature (Razmjou *et al*. 2012):

$$LEP = \frac{-2\beta\gamma_{lv}\ Cos\ \theta}{r_{max}} \qquad (3)$$

where, β is a pore geometry factor (β ranges 1 to 0.5 for cylindrical spherical pore, γ_{lv} is the liquid−vapor surface tension of the wetting phase, r_{max} is maximum pore radius and θ is surface contact angle. The theoretical LEP is estimated using Eq. (3) and compared with the experimental measured LEP as shown in Table 3. It can be illustrated from Table 3, that on increasing the coagulant concentration from 0 to 100 % ethanol, the LEP increased from 92.10 kPa to 189.92 kPa. This increase in LEP can be explained due to morphological changes on membrane surface and increase in hydrophobicity of the membrane on increasing ethanol concentration in the coagulation bath. CBC-0 membrane has a finger-like structure and wide pores as compared to CBC-100 membrane, therefore with decrease in pore size, the LEP of the membrane increases as it is inversely proportional to the maximum pore size of the membrane whereas the value of β value is higher for cylindrical pores as compared to spherical) pore size which in turn decreases the LEP value on increasing the ethanol concentration from 0 to 100 %. It is evident that overall percentage contribution of pore size and hydrophobicity affected LEP in positive direction and dominate the negative effect of pore geometry factor β on LEP. Moreover, it was also observed that theoretical LEP is lower than its experimental LEP value. This is quite obvious because experimental LEP was estimated with support of nonwoven fabric in MD module.

3.3 Effect of coagulation bath concentration on porosity and tensile strength

From the previous section, it was understood that on increasing the ethanol concentration in the bath, the

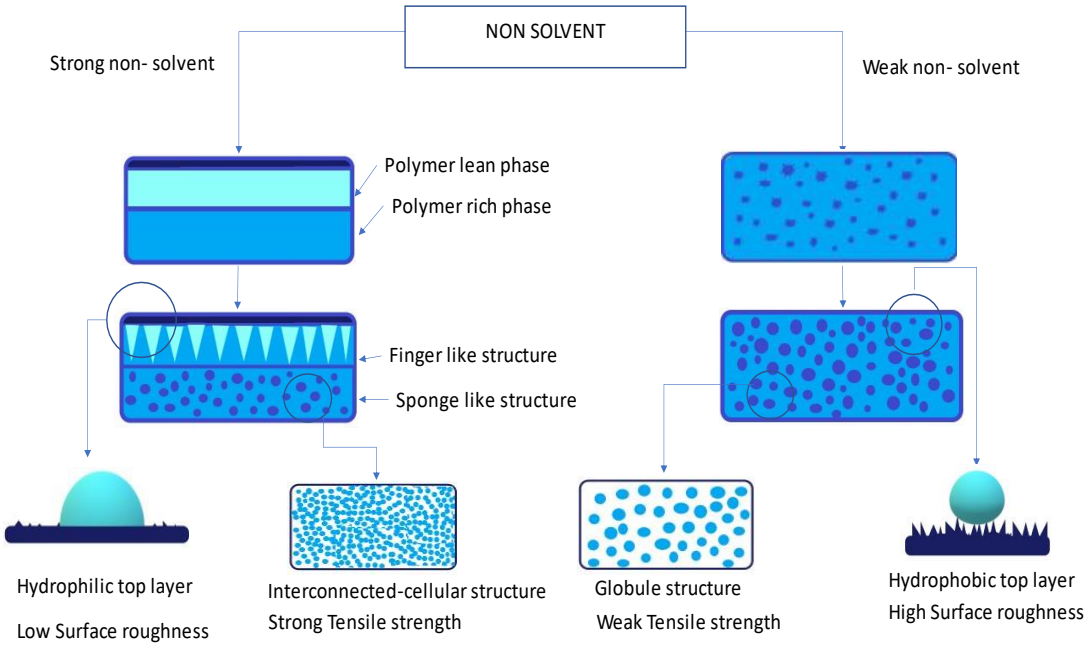

Fig. 5 Effect of non-solvent on membrane morphology, membrane hydrophobicity and microstructural morphology

Table 4 Porosity and tensile strength of 16 wt% PVDF membrane

Membrane code	Membrane Porosity (%)	Tensile Strength (MPa)
CBC-0	52.58	203.2
CBC-15	53.40	198.1
CBC- 30	54.31	197.5
CBC- 45	55.29	182.5
CBC- 60	55.87	180
CBC-75	56.45	174.3
CBC-100	57.37	162.5

demixing rate of solvent and non-solvent decreases, which results in the formation of many nuclei on the top surface, probably occurred due to the presence of a degree of supersaturation for PVDF crystallization which depressed the liquid-liquid demixing as a result polymerization of polymer in the film dominates. These changes in the polymer structure not only affect the contact angle but also other properties such as membrane porosity and membrane tensile strength. Therefore, the fabricated flat sheet PVDF membrane using NIPS under various bath compositions was examined for porosity and tensile strength. Table 3, represents the effect of coagulation bath composition as prescribed in Table 1 on membrane porosity and tensile strength. From this table, it is observed that the porosity of the membrane does not change significantly by changing the coagulation bath concentration. The porosity of the PVDF membrane prepared with pure water as a coagulant is found to be 52.58%, whereas it is 57.37 % at a coagulation bath concentration of 100 wt % ethanol. This slight increase in porosity may be due to a change in hydrodynamic behaviour during mass transfer between the solvent-nonsolvent. Basically, the liquid-liquid exchange rate dropped and the membrane formation took a long time, creating a more symmetric structure where macro voids gradually disappeared on increasing the ethanol concentration in the bath. Despite the depression of the macro void structure of the membrane due to the reduced mass exchange rate, the porosity of the membrane increases because a totally symmetric membrane with well interconnected small dimensional spherulites micropores were formed on account of gradual but continuous mass transfer. It is noteworthy that during delayed demixing (higher ethanol concentration), small micropores are formed at the top layer hence porosity of the membrane matrix increases as compared to fast demixing (lower ethanol concentration).

Since porosity and tensile strength of membrane are interrelated to each other. Therefore, the tensile strength of the prepared PVDF hydrophobic membrane was determined using UTM. It is observed in Table 3, the tensile strength of the fabricated membrane decreased from 203.2 to 162.5 MPa on increasing the coded bath composition from CBC-0 to CBC-100 respectively. This can be attributed to observing the cross-section morphology under high magnifications (5000X), as shown in Fig. 2. It is apparent from Fig. 2, that the membrane structure is gradually transformed from an interconnected-cellular type to an interconnected-globule transition type and finally a globule type structure. This change in the structure of the membrane from particulate morphology to globules type morphology limits the linking points between the globules and the structure became more loosely packed. This leads to a decrease in the mechanical strength of the membrane. This implicit understanding of the overall effect of non-solvent on overall membrane morphology and its properties can be explicit using the picture represented in Fig. 5. When strong non-solvent (water) is used as a coagulant, fabricated

membrane divides into two phases, polymer-rich and polymer lean and asymmetric membrane with finger and sponge-like structure was formed, whereas, for weak non solvent such as ethanol, sponge-like morphology was observed throughout. Particulate morphology of membrane changes from interconnected-cellular type to an interconnected-globule with an increase in ethanol in non-solvent, which in turn reduces the mechanical strength. An increase in hydrophobicity of the membrane with ethanol concentration is also represented in the pictorial presentation in Fig. 5.

4. Conclusions

PVDF flat sheet hydrophobic membranes were prepared using the phase inversion technique suitable for membrane distillation application. The effect of different non-solvents (water and ethanol) individually and their synergistic composition on membrane morphology as well as other prime characteristics of the membrane were studied.

• It was found that week non-solvent, ethanol when used in the membrane synthesis process during coagulation, increases the porosity and hydrophobicity of the membrane along with the formation of smaller pore size with a higher contact angle of the membrane.

• On increasing the ethanol concentration from 0 to 100% in a coagulant bath morphology of the membrane changes from finger-like morphology to a sponge-like structure.

It was found that the contact angle and porosity of the membrane along with other characteristics were in the desired range for various MD applications.

References

Abdel-karim, A., Leaper, S., Alberto, M., Vijayaraghavan, A., Fan, X., Holmes, S.M., Souaya, E.R., Badawy, M.I. and Gorgojo, P. (2018), "High flux and fouling resistant flat sheet polyethersulfone membranes incorporated with graphene oxide for ultra filtration applications", *Chem. Eng. J.*, **334**, 789-799. https://doi.org/10.1016/j.cej.2017.10.069.

Baghel, R., Upadhyaya, S., Singh, K. and Chaurasia, S.P. (2017), "A review on membrane applications and transport mechanisms in vacuum membrane distillation", *Rev. Chem. Eng.*, **34**(1), 73-106. https://doi.org/10.1515/revce-2016-0050.

Baghel, R., Kalla, S., Upadhyaya, S., Chaurasia, S.P. and Singh, K. (2020), "Chemical Engineering Research and Design CFD modeling of vacuum membrane distillation for removal of Naphthol blue black dye from aqueous solution using COMSOL multiphysics", *Chem. Eng. Res. Des.*, **158**, 77-88. https://doi.org/10.1016/j.cherd.2020.03.016.

Chang, H.H., Tsai, C.H., Wei, H.C. and Cheng, L.P. (2014), "Effect of structure of PVDF membranes on the performance of membrane distillation", *Membr. Water Treat.*, **5**(1), 41-56. https://doi.org/10.12989/MWT.2014.5.1.041

Deshmukh, S.P. and Li, K. (1998), "Effect of ethanol composition in water coagulation bath on morphology of PVDF hollow fibre membranes", *J. Membr. Sci.*, **150**(1), 75-85. https://doi.org/10.1016/S0376-7388(98)00196-3.

Essalhi, M. and Khayet, M. (2012), "Surface segregation of fluorinated modifying macromolecule for hydrophobic/ hydrophilic membrane preparation and application in air gap and direct contact membrane distillation", *J. Membr. Sci.*, **417-418**, 163-173, https://doi.org/10.1016/j.memsci.2012.06.028.

Garcia-Payo, M.C., Essalhi, M., Khayet, M., Garcia-Fernandez, L., Charfi, K. and Arafat, H. (2010), "Water desalination by membrane distillation using PVDF-HFP hollow fiber membranes", *Membr. Water Treat.*, **1**(3), 215-230. https://doi.org/10.12989/MWT.2010.1.3.215

Gholami, A., Moghadassi, A. R., Hosseini, S. M., Shabani, S. and Gholami, F. (2013), "Preparation and characterization of polyvinyl chloride based nanocomposite nanofiltration- membrane modified by iron oxide nanoparticles for lead removal from water", *J. Ind. Eng. Chem.*, 6-11, https://doi.org/10.1016/j.jiec.2013.07.041.

Gryta, M. (2010), "Application of membrane distillation process for tap water purification", *Membr. Water Treat.*, **1**(1), 1-12. https://doi.org/10.12989/MWT.2010.1.1.001

Haan, T.Y., Shah, M., Chun, H.K. and Mohammad, A.W. (2018). "A study on membrane technology for surface water treatment: Synthesis, characterization and performance test", *Membr. Water Treat.*, **9**(2), 69-77. https://doi.org/10.12989/MWT.2018.9.2.069

Hou, D., Wang, J., Qu, D., Luan, Z. and Ren, X. (2009), "Fabrication and characterization of hydrophobic PVDF hollow fiber membranes for desalination through direct contact membrane distillation", *Sep. Purif. Technol.*, **69**(1), 78-86. https://doi.org/10.1016/j.seppur.2009.06.026.

Kotsilkova, R., Borovanska, I., Todorov, P., Ivanov, E., Menseidov, D., Chakraborty, S. and Bhattacharjee, C. (2018), "Tensile and Surface Mechanical Properties of Polyethersulphone (PES) and Polyvinylidene Fluoride (PVDF) Membranes", *J. Theor. Appl. Mech.*, **48**(3), 85-99, https://doi.org/10.2478/jtam-2018-0018.

Li, Q., Xu, Z.L. and Liu, M. (2011), "Preparation and characterization of PVDF microporous membrane with highly hydrophobic surface", *Polym. Adv. Technol.*, **22** (5), 520-531. https://doi.org/10.1002/pat.1549.

Macedonio, F. and Drioli, E. (2010), "Membrane engineering progresses in desalination and water reuse", *Membr. Water Treat.*, **1**(1), 75-81. https://doi.org/10.12989/MWT.2010.1.1.075.

Munirasu, S., Banat, F., Ahmed, A. and Abu, M. (2017), "Intrinsically superhydrophobic PVDF membrane by phase inversion for membrane distillation", *Desalination* ,**417**, 77-86. https://doi.org/10.1016/j.desal.2017.05.019.

Pagliero, M., Bottino, A., Comite, A. and Costa, C. (2020), "Novel hydrophobic PVDF membranes prepared by nonsolvent induced phase separation for membrane distillation", *J. Membr. Sci.*, **596**, 117575. https://doi.org/10.1016/j.memsci.2019.117575.

Peydayesh, M., Mohammadi, T. and Kordmirza, S. (2020), "A positively charged composite loose nanofiltration membrane for water purification from heavy metals", *J. Membr. Sci.*, **611**, 118205. https://doi.org/10.1016/j.memsci.2020.118205.

Razmjou, A., Arifin, E., Dong, G.,Mansouri, J. and Chen, V. (2012), "Superhydrophobic modification of TiO2 nanocomposite PVDF membranes for applications in membrane distillation", *J. Membr. Sci.*, **415-416**, 850-863. https://doi.org/10.1016/j.memsci.2012.06.004.

Singh, J.K., Upadhyaya, S., Chaurasia, S.P. and Baghel, R. (2017), "Study on membrane fouling in vacuum membrane distillation for desalination", *J. Basic Appl. Eng. Res.*, **4**(3), 229-233.

Sui, Y., Wang, Z., Gao, X. and Gao, C. (2012), "Antifouling PVDF ultrafiltration membranes incorporating PVDF-g-PHEMA additive via atom transfer radical graft polymerizations", *J. Membr. Sci.*, **413-414**, 38-47. https://doi.org/10.1016/j.memsci.2012.03.055.

Sukitpaneenit, P. and Chung, T.S. (2009), "Molecular elucidation

of morphology and mechanical properties of PVDF hollow fiber membranes from aspects of phase inversion, crystallization and rheology", *J. Membr. Sci.*, **340**(1-2), 192-205. https://doi.org/10.1016/j.memsci.2009.05.029.

Tae, J., Kim, J.F., Hyun, H., Drioli, E. and Moo, Y. (2016), "Understanding the non-solvent induced phase separation (NIPS) effect during the fabrication of microporous PVDF membranes via thermally induced phase separation (TIPS)", *J. Membr. Sci.*, **514**, 250-263. https://doi.org/10.1016/j.memsci.2016.04.069.

Tibi, F., Charfi, A., Cho, J. and Kim, J. (2020), "Fabrication of polymeric membranes for membrane distillation process and application for wastewater treatment: Critical review", *Proc. Safe. Environ. Protect.*, **141**, 190-201. https://doi.org/10.1016/j.psep.2020.05.026.

Upadhyaya, S., Singh, K., Chaurasia, S.P., Dohare, R.K. and Agarwal, M. (2016), "Mathematical and CFD modeling of vacuum membrane distillation for desalination", *Desalin. Water Treat.*, **57**(26), 11956-11971. https://doi.org/10.1080/19443994.2015.1048306a.

Upadhyaya, S., Singh, K., Chaurasia, S.P. and Dohare, R.K. (2016), "Recovery and development of correlations for heat and mass transfer in vacuum membrane distillation for desalination", *Desalin. Water Treat.*, 3994. https://doi.org/10.1080/19443994.2016.1189245b.

Xu, K., Cai, Y., Tavajohi, N., Cheng, Y., Li, X. and Wang, X. (2019), "ECTFE membrane fabrication via TIPS method using ATBC diluent for vacuum membrane distillation", *Desalination*, **456**, 13-22. https://doi.org/10.1016/j.desal.2019.01.004.

Yadav, M., Upadhyaya, S., Singh, K. and Vashishtha, M., (2021), "Morphological study of fabricated PVDF based hydrophobic membrane for different additives and coagulation bath temperature", *Asian J. Water Environ. Pollut.*, **18**(3), 39-47. https://doi.org/10.3233/AJW210027.

Zahirifar, J., Moosavian, S.M.A., Hadi, A., Khadiv-Parsi, P. and Karimi-Sabet, J. (2018), "Fabrication of a novel octadecylamine functionalized graphene oxide/PVDF dual-layer flat sheet membrane for desalination via air gap membrane distillation", *Desalination*, **428**, 227-239. https://doi.org/10.1016/j.desal.2017.11.028.

Zhang, J., Li, J. and Gray, S. (2011), "Effect of applied pressure on performance of PTFE membrane in DCMD", *J. Membr. Sci.*, **369**(1-2), 514-525. https://doi.org/10.1016/j.memsci.2010.12.033.

Zhu, H., Wang, H., Wang, F., Guo, Y., Zhang, H. and Chen, J. (2013), "Preparation and properties of PTFE hollow fiber membranes for desalination through vacuum membrane distillation", *J. Membr. Sci.*, **446**, 145-153. https://doi.org/10.1016/j.memsci.2013.06.037.

KC